

BASIC RESEARCH PAPER

Role for DUSP1 (dual-specificity protein phosphatase 1) in the regulation of autophagy

Juan Wang^{a,b}, Jun-Ying Zhou^{a,b}, Dhonghyo Kho^{a,b}, John J. Reiners, Jr.^{a,c}, and Gen Sheng Wu^{a,b}

^aMolecular Therapeutics Program, Karmanos Cancer Institute, Wayne State University School of Medicine, Detroit, MI, USA; ^bDepartments of Oncology and Pathology, Wayne State University School of Medicine, Detroit, MI, USA; ^cInstitute of Environmental Health Sciences, Wayne State University, Detroit, MI, USA

ABSTRACT

Accumulating evidence suggests that mitogen-activated protein kinases (MAPKs) regulate macroautophagy/autophagy. However, the involvement of dual-specificity protein phosphatases (DUSPs), endogenous inhibitors for MAPKs, in autophagy remains to be determined. Here we report that DUSP1/MKP-1, the founding member of the DUSP family, plays a critical role in regulating autophagy. Specifically, we demonstrate that *DUSP1* knockdown by shRNA in human ovarian cancer CAOV3 cells and knockout in murine embryonic fibroblasts, increases both basal and rapamycin-increased autophagic flux. Overexpression of *DUSP1* had the opposite effect. Importantly, knockout of *Dusp1* promoted phosphorylation of ULK1 at Ser555, and BECN1/Beclin 1 at Ser15, and the association of PIK3C3/VPS34, ATG14, BECN1 and MAPK, leading to the activation of the autophagosome-initiating class III phosphatidylinositol 3-kinase (PtdIns3K) complex. Furthermore, knockdown and pharmacological inhibitor studies indicated that DUSP1-mediated suppression of autophagy reflected inactivation of the MAPK1-MAPK3 members of the MAPK family. Knockdown of *DUSP1* sensitized CAOV3 cells to rapamycin-induced antigrowth activity. Moreover, CAOV3-CR cells, a line that had acquired cisplatin resistance, exhibited an elevated DUSP1 level and were refractory to rapamycin-induced autophagy and cytostatic effects. Knockdown of *DUSP1* in CAOV3-CR cells restored sensitivity to rapamycin. Collectively, this work identifies a previously unrecognized role for DUSP1 in regulating autophagy and suggests that suppression of DUSP1 may enhance the therapeutic activity of rapamycin.

ARTICLE HISTORY

Received 26 May 2015
Revised 31 May 2016
Accepted 14 June 2016

KEYWORDS

autophagy; cisplatin resistance; DUSP1
MAPK/ERK; ovarian cancer

Introduction

Autophagy is a highly conserved process by which cytoplasmic materials are encapsulated in double-membrane compartments, phagophores, that mature into autophagosomes, allowing the subsequent degradation of the cargo following fusion of the latter with lysosomes.¹ Autophagy is a constitutive process and plays a critical role in the degradation of long-lived proteins and aged/dysfunctional organelles. However, autophagy is also induced by nutrient and energy deficiency, and as a response to cellular damage induced by a variety of exogenous stressors.^{1,2} As such, constitutive and inducible autophagy has critical roles in cellular housekeeping and maintenance of homeostasis. Although generally viewed as being a prosurvival process, there are numerous cases in which autophagy appears to directly mediate or contribute to cell death.^{3,4} Extensive literature documents the prosurvival functions of autophagy, and the induction of autophagy in tumors during chemotherapy often provides a survival advantage,^{5,6} but there are cases in which autophagy mediates the cytotoxic effects of stressors and therapeutics, and promoting autophagy causes cancer cell death or sensitizes cancer cells to other chemotherapeutics.^{3,4} In addition, autophagy is increasingly recognized as a critical player in cancer development, but its role in cancer is complex. For example, mutations resulting in the loss or silencing of *Becn1* or *Atg5* are pro-tumorigenic, and

can promote chromosome rearrangements and aneuploidy.⁷⁻⁹ Similarly, autophagy occurring in cancer-associated stromal cells can promote the survival and growth of neighboring tumors.^{10,11}

Mammalian MAPKs mainly consist of MAPK8/JNK1, MAPK9/JNK2, MAPK10/JNK3, MAPK11/p38 β , MAPK12/p38 γ , MAPK13/p38 δ , MAPK14/p38 α , MAPK1/ERK2, and MAPK3/ERK1 (hereafter referred to primarily as MAPK/JNK, MAPK/p38 and MAPK/ERK, respectively),^{12,13} each of which are activated by diverse stimuli. In response to stimuli, MAPKs are activated through the reversible phosphorylation of both threonine and tyrosine residues of the TXY motif in the catalytic domain by upstream dual-specificity kinases. These upstream kinases, named MAP kinase kinases (MKKs/MEKs), include MAP2K1/MKK1, MAP2K2/MKK2, MAP2K3/MKK3, MAP2K4/MKK4, MAP2K6/MKK6 and MAP2K7/MKK7, which are in turn activated by MAPK kinase kinases.¹⁴⁻¹⁶ Activated MAPKs phosphorylate a number of substrates and subsequently modulate many signaling pathways and processes including autophagy.^{15,17-19}

Since phosphorylation is required for the activation of MAPKs, dephosphorylation by members of the DUSP (dual-specificity protein phosphatase) family plays a critical role in controlling MAPK signaling. The DUSP family contains 11 members, including DUSP1, DUSP2, DUSP4, DUSP5, DUSP6, DUSP7, DUSP8, DUSP9, DUSP10, DUSP16 and STYXL1.²⁰

CONTACT Gen Sheng Wu ✉ wug@karmanos.org Molecular Therapeutics Program, Karmanos Cancer Institute, Departments of Oncology and Pathology, Wayne State University School of Medicine, Detroit, MI 48201, USA.

Color versions of one or more of the figures in the article can be found online at www.tandfonline.com/kaup.

DUSP1 is the founding member of the DUSP family and was originally identified as a growth factor and stress inducible gene.²¹⁻²⁴ DUSP1 is a dual-specificity protein phosphatase that dephosphorylates both the threonine and tyrosine residues on members of all 3 major MAPK subfamilies—MAPK/JNK, MAPK/p38, and MAPK/ERK.²⁵⁻²⁷ DUSP1 is involved in the regulation of the cell cycle and apoptosis.²⁸⁻³³ Importantly, DUSP1 is overexpressed in several cancers, including ovarian cancer.³⁴⁻³⁶ DUSP1 inhibits the induction of cell death by several apoptotic stimuli.^{31,33,37,38} Furthermore, studies with lung and ovarian cancer cells demonstrate a clear correlation between increased DUSP1 expression and acquired chemoresistance.^{33,38} Furthermore, studies have shown that DUSP1 can protect cells from chemotherapy-induced apoptosis.³⁷ However, it is not known whether DUSP1 plays a role in autophagy.

In this study we investigated the effects of *DUSP1* knockdown and overexpression on basal and rapamycin-induced autophagy in 3 different cellular models. In all 3 models both basal and inducible autophagic activities were inversely related to DUSP1 level. The effects of DUSP1 were primarily due to its inactivation of MAPK/ERK, which positively regulated autophagy. We also evaluated the therapeutic use of rapamycin to treat human ovarian cancer cells. Rapamycin significantly reduced proliferation via a mechanism that was dependent upon the induction of autophagy. However, sensitivity to rapamycin was significantly compromised in variant ovarian cancer cells that were unable to mount an autophagic response due to the upregulated expression of DUSP1.

Results

Knockdown or knockout of *DUSP1* leads to an increase in MAP1LC3-II/LC3-II levels whereas its overexpression has an opposite effect

MAP1LC3/LC3 is a cytosolic protein that is incorporated into the membranes of phagophores. Prior to its incorporation, LC3-I is converted into LC3-II by a post-translational modification in which phosphatidylethanolamine is covalently attached. Cellular LC3-II content is commonly used as a marker of autophagy and as an index of autophagosome formation.² CAOV3 ovarian cancer cells exhibited basal expression of LC3-II (Fig. 1A). Knockdown of *DUSP1* in CAOV3 cells increased LC3-II levels (Fig. 1A). In order to determine if the observed result was cell-line specific, we analyzed LC3-II levels in 2 additional model systems. Like *DUSP1* knockdown CAOV3 cells, LC3-II levels were greater in *dusp1*^{-/-} mouse embryonic fibroblasts (MEFs) derived from *Dusp1* knockout mice, relative to MEFs derived from wild-type mice (Fig. 1B). Conversely, *DUSP1*-overexpressing human ovarian cancer TOV112D cells exhibited lower LC3-II levels than empty vector control cells (Fig. 1C).

To further confirm the role of DUSP1 in regulating LC3-II levels, we treated nontarget shRNA control and *DUSP1* knockdown CAOV3 cells with rapamycin, a well-characterized inducer of autophagy.^{2,39} Figure 1D shows that both basal and rapamycin-induced LC3-II levels were higher in *DUSP1* knockdown cells. Furthermore, SQSTM1/p62 levels were decreased

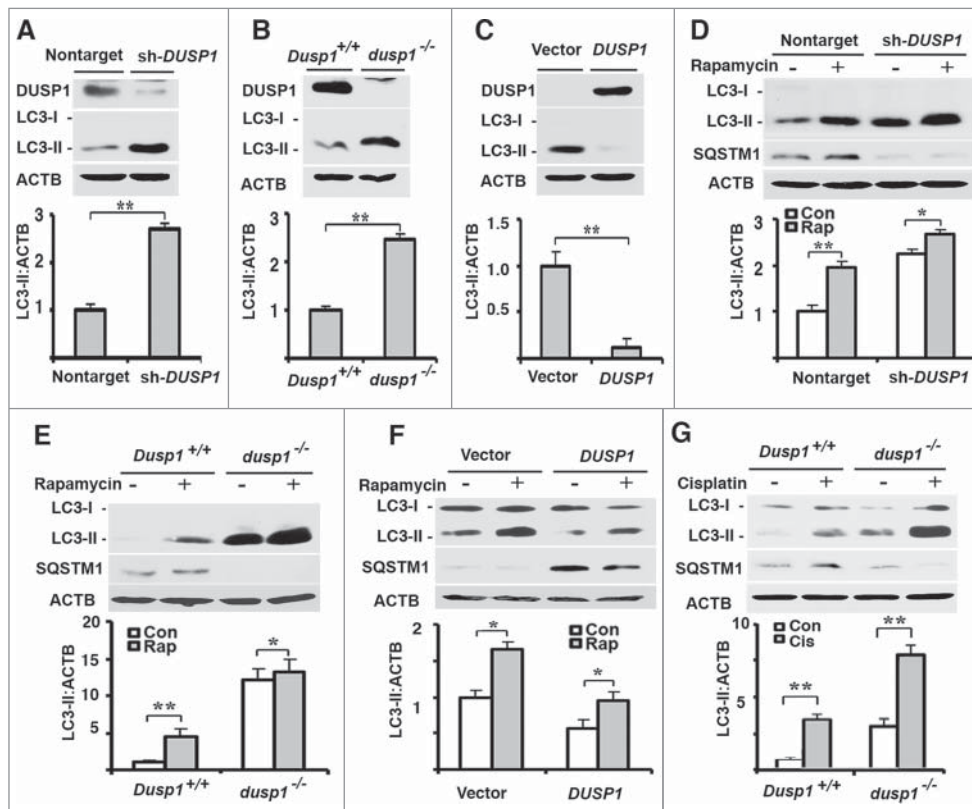


Figure 1. Correlations between DUSP1, LC3-II and SQSTM1 levels. Western blot analyses of DUSP1, LC3-I, LC3-II, ACTB or SQSTM1 (upper panel) and quantification of LC3-II (lower panel) in (A and D) CAOV3 cells stably transfected with *DUSP1* shRNA (sh-*DUSP1*) or nontarget control shRNA (Nontarget), (B, E and G) *Dusp1*^{+/+} and *dusp1*^{-/-} MEFs, and (C and F) TOV112D cells stably transfected with *DUSP1* cDNA or empty vector. Cells (D-F) were left untreated or treated with 5 μ M rapamycin (Rap) for 20 h prior to being harvested for western blot analyses. Cells (G) were left untreated or treated with 20 μ M cisplatin for 24 h prior to being harvested for western blot analysis. Data represent mean \pm SD of 3 independent experiments. *, P < 0.01 and **, P < 0.005, statistically significant.

in *DUSP1* knockdown cells (Fig. 1D). This is significant because SQSTM1 is involved in autophagic degradation of protein aggregates and damaged mitochondria, and reductions in SQSTM1, coupled with increased LC3-II levels, are indicative of functional autophagy.² Similar results were obtained in *dusp1*^{-/-} MEFs (Fig. 1E), and opposite results were obtained in *DUSP1*-overexpressing TOV112D cells (Fig. 1F). Importantly, an inverse relationship between functional autophagy and *DUSP1* level was also observed in *Dusp1*^{+/+} and *dusp1*^{-/-} MEFs following treatment with cisplatin (Fig. 1G), another

inducer of autophagy.⁴⁰ Taken together, these data suggest that *DUSP1* may negatively regulate autophagy.

To further define the role of *DUSP1* in regulating autophagy, we used multiple approaches to monitor autophagosome development/accumulation. The first approach employed fluorescence microscopy to assess the incorporation of stably expressed GFP-LC3 into fluorescent punctate structures (Fig. 2A-C). Fluorescent GFP-LC3 puncta were relatively absent in untreated nontarget shRNA CAOV3 cells (Fig. 2A) and wild-type *Dusp1*^{+/+} MEFs (Fig. 2B), but apparent in rapamycin-treated cells. In

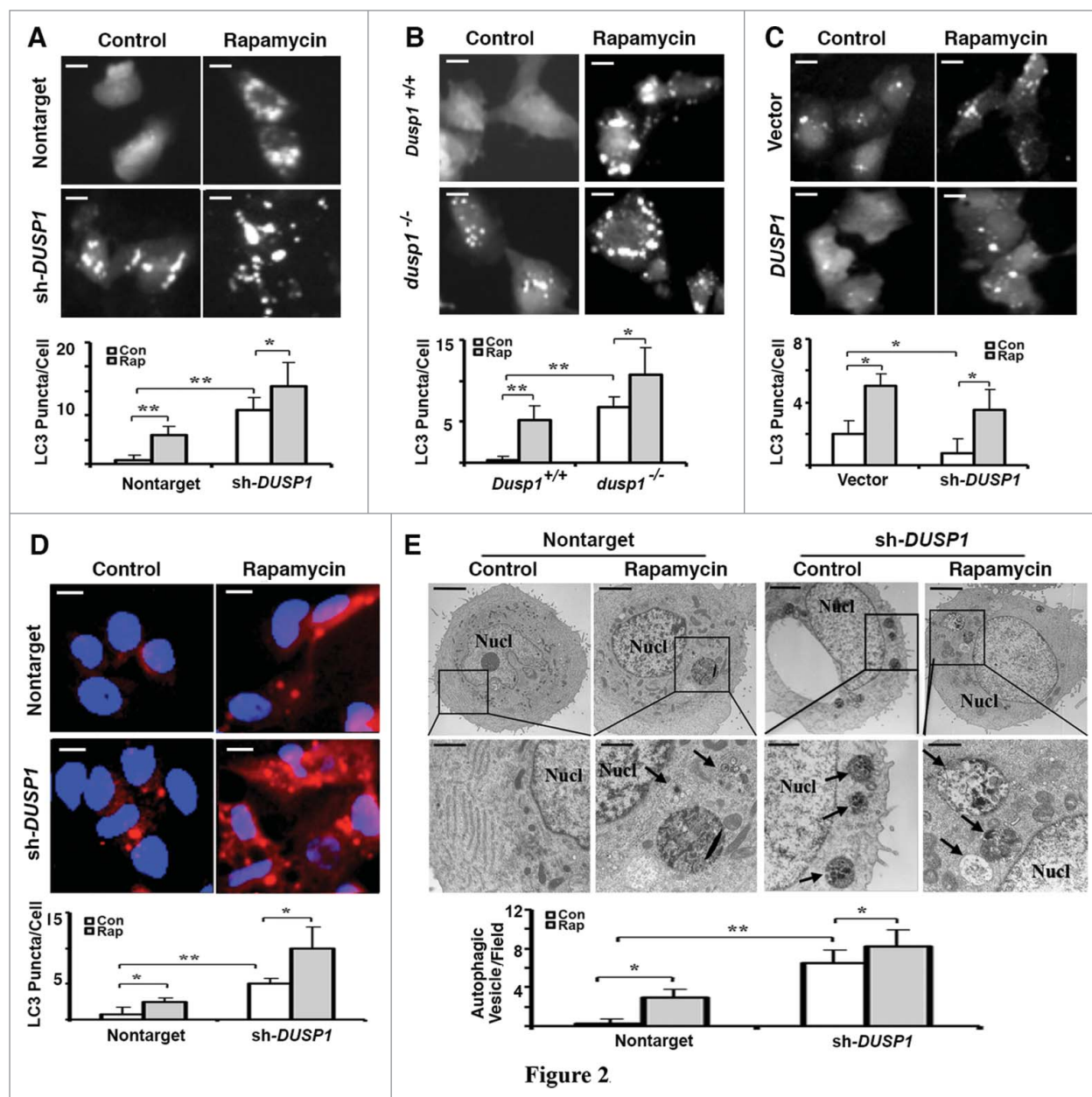


Figure 2

Figure 2. Inverse relationship between *DUSP1* expression and autophagic vesicle formation. (A-C) Representative fluorescence images (upper panels) and quantification of GFP-LC3 puncta (lower panels) in (A) CAOV3 cells with *DUSP1* shRNA (sh-*DUSP1*) or nontarget shRNA, (B) *Dusp1*^{+/+} and *dusp1*^{-/-} MEFs and (C) TOV112D cells stably transfected with *DUSP1* cDNA or empty vector. Cells were left untreated or treated with 5 μ M rapamycin for 20 h prior to image capture. Bright puncta denote autophagosomal structures. (D) Representative indirect immunofluorescent images of endogenous LC3. *DUSP1* shRNA or nontarget shRNA CAOV3 cells were left untreated or treated with 5 μ M rapamycin for 20 h prior to being processed for immunofluorescent detection of LC3. Red puncta denote autophagic vesicle structures (upper panel) and quantification of LC3 puncta (lower panel). Data represent mean \pm SD of 3 independent experiments, in each of which 20 or more cells were counted. (E) Representative electron micrographs (upper panel) and quantification of autophagic vesicles (lower panel). *DUSP1* shRNA or nontarget shRNA CAOV3 cells were left untreated or treated with rapamycin (5 μ M, 20 h). Arrows denote autophagic vesicles. Nucl, nucleus. Scale bars: (A-D) 10 μ m; (E) 1.7 μ m (upper panels), 600 nm (lower panels). *, $P < 0.01$ and **, $P < 0.005$, statistically significant.

contrast, fluorescent GFP-LC3 puncta were easily observed in untreated *DUSP1* knockdown CAOV3 (Fig. 2A) and *dusp1*^{-/-} MEF (Fig. 2B) cells, and increased in number following rapamycin treatment (Fig. 2A, B). This indicates that knockdown of *DUSP1* increases autophagosome accumulation. Conversely, GFP-LC3 fluorescence was primarily punctate in nontreated vector control TOV112D cells, but mostly diffuse and non-punctate in *DUSP1*-overexpressing TOV112D cells (Fig. 2C). Although rapamycin treatment enhanced the conversion of GFP-LC3 into fluorescent puncta in *DUSP1*-overexpressing TOV112D cells, there was still considerable diffuse cytoplasmic fluorescence (Fig. 2C). In addition, we used antibodies to LC3 and indirect immunofluorescence to monitor endogenous LC3 incorporation into puncta in CAOV3 cells stably expressing nontarget control shRNA or *DUSP1* shRNA (Fig. 2D). Untreated nontarget shRNA CAOV3 cells exhibited few LC3 puncta, which increased after treatment with rapamycin (Fig. 2D). In contrast, endogenous LC3 puncta were easily observed in *DUSP1* knockdown cells in the absence of rapamycin treatment, and markedly increased following rapamycin treatment (Fig. 2D). Finally, we used transmission electron microscopy to determine if organelles consistent with autophagosomes could be identified, and if their abundance correlated with our proxy (*i.e.*, LC3-II, GFP-LC3 puncta) measurements of autophagy. Vesicles with double membranes, a structural feature unique to autophagosomes, were easily

observed and abundant in both nontreated and rapamycin-treated *DUSP1* knockdown CAOV3 cells (Fig. 2E). In contrast, autophagic vesicles were markedly fewer in nontarget shRNA-expressing CAOV3 cells (Fig. 2E). Taken together, these data strongly suggest that *DUSP1* negatively regulates both constitutive and inducible autophagy.

The cellular LC3-II level reflects not only the rate of autophagosome formation, but also the efficiencies of autophagosome fusion with lysosomes, and subsequent lysosomal degradation of LC3-II.² In order to determine if the observed inverse relationship between LC3-II and *DUSP1* levels reflected effects on autophagosome maturation, we treated cells with bafilomycin A₁ (BafA₁), which inhibits both autophagosome-lysosome fusion and lysosome-mediated degradation of fused autophagosomes and their cargo.⁴¹ If LC3-II levels are similar in BafA₁-treated and nontreated cells, such results are generally interpreted as a block in autophagosome maturation/degradation and an inhibition of autophagic flux. Conversely, normal autophagic flux is assumed if BafA₁ treatment increases LC3-II levels. Furthermore, if BafA₁-treatment enhances the accumulation of LC3-II above what is observed following some treatment/manipulation, it is assumed that the increased LC3-II accumulation occurring as a consequence of the treatment/manipulation reflects increased autophagosome formation. Treatment of CAOV3 (Fig. 3A), MEF (Fig. 3B) and TOV112D (Fig. 3C) cells with BafA₁ increased both basal and rapamycin-

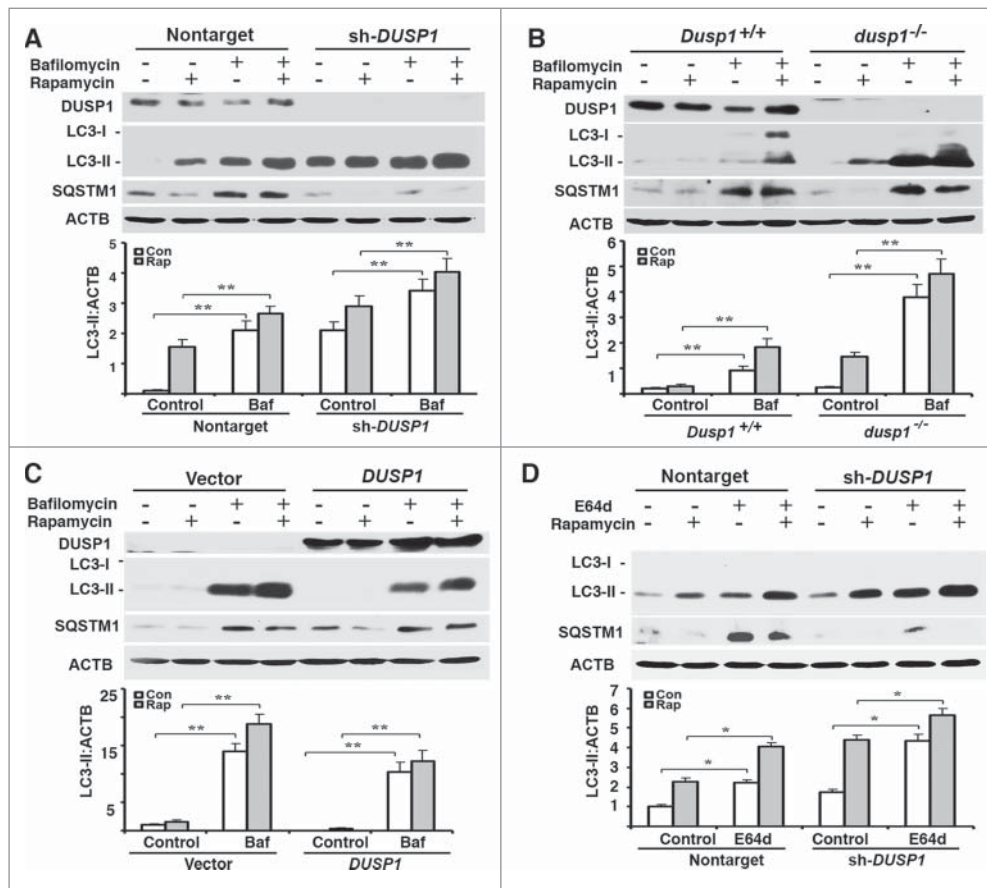


Figure 3. Effects of *DUSP1* on autophagic flux. (A–D) Western blot analyses of *DUSP1*, LC3, SQSTM1 and ACTB (upper panel) and quantification of LC3 (lower panel). (A and D) *DUSP1* shRNA (sh-*DUSP1*) or nontarget shRNA CAOV3 cells. (B) *Dusp1*^{+/+} and *dusp1*^{-/-} MEFs. (C) Stable *DUSP1* overexpression and empty vector control TOV112D cells. Cells were left untreated, or treated with 5 μ M rapamycin and/or 10 nM bafilomycin A₁ (A–C) or 10 μ g/ml E64d (D) for 20 h before being harvested for western blot analyses. Data represent mean \pm SD of 3 independent experiments. *, $P < 0.01$ and **, $P < 0.005$, statistically significant.

induced LC3-II levels, as well as basal SQSTM1 levels. These effects of BafA₁ were independent of DUSP1 level (Fig. 3A-C). However, greater accumulations of LC3-II always occurred in DUSP1-deficient cells (Fig. 3A-C). Similar results were obtained in CAOV3 cells treated with the lysosomal protease inhibitor E64d (Fig. 3D). Collectively, these data suggest that autophagosome formation and flux are increased in DUSP1-deficient cells.

DUSP1 inhibits MAPK/ERK-mediated autophagy

Given that phospho-MAPKs are the only known substrates of DUSP1,^{35,42} it seemed logical that the effects of DUSP1 deficiency had to be related to the activities of one or more of these MAPKs. Figure 4A shows that DUSP1-deficient CAOV3 cells,

relative to cells transfected with nontarget shRNA, exhibited higher basal levels of phosphorylated (activated) MAPKs. Interestingly, treatment of DUSP1-deficient CAOV3 cells with rapamycin decreased basal phosphorylated MAPK/JNK and MAPK/p38, without having an obvious effect on MAPK/ERK phosphorylation (Fig. 4A). To address whether MAPK/ERK plays a role in DUSP1 modulation of autophagy, *dusp1*^{-/-} MEFs were left untreated, or treated with the MAPK/p38 inhibitor SB203580, the MAPK/JNK inhibitor SP600125, or the MAP2K inhibitor U0126 for 24 h. Each agent suppressed the phosphorylation of its respective kinase target (Fig. 4B). Whereas SP600125 had marginal effects on basal LC3-II levels, the MAPK/p38 and MAPK/ERK inhibitors markedly enhanced and reduced, respectively, basal LC3-II levels (Fig. 4B). Furthermore, the MAPK/ERK inhibitor U0126 reduced both basal and

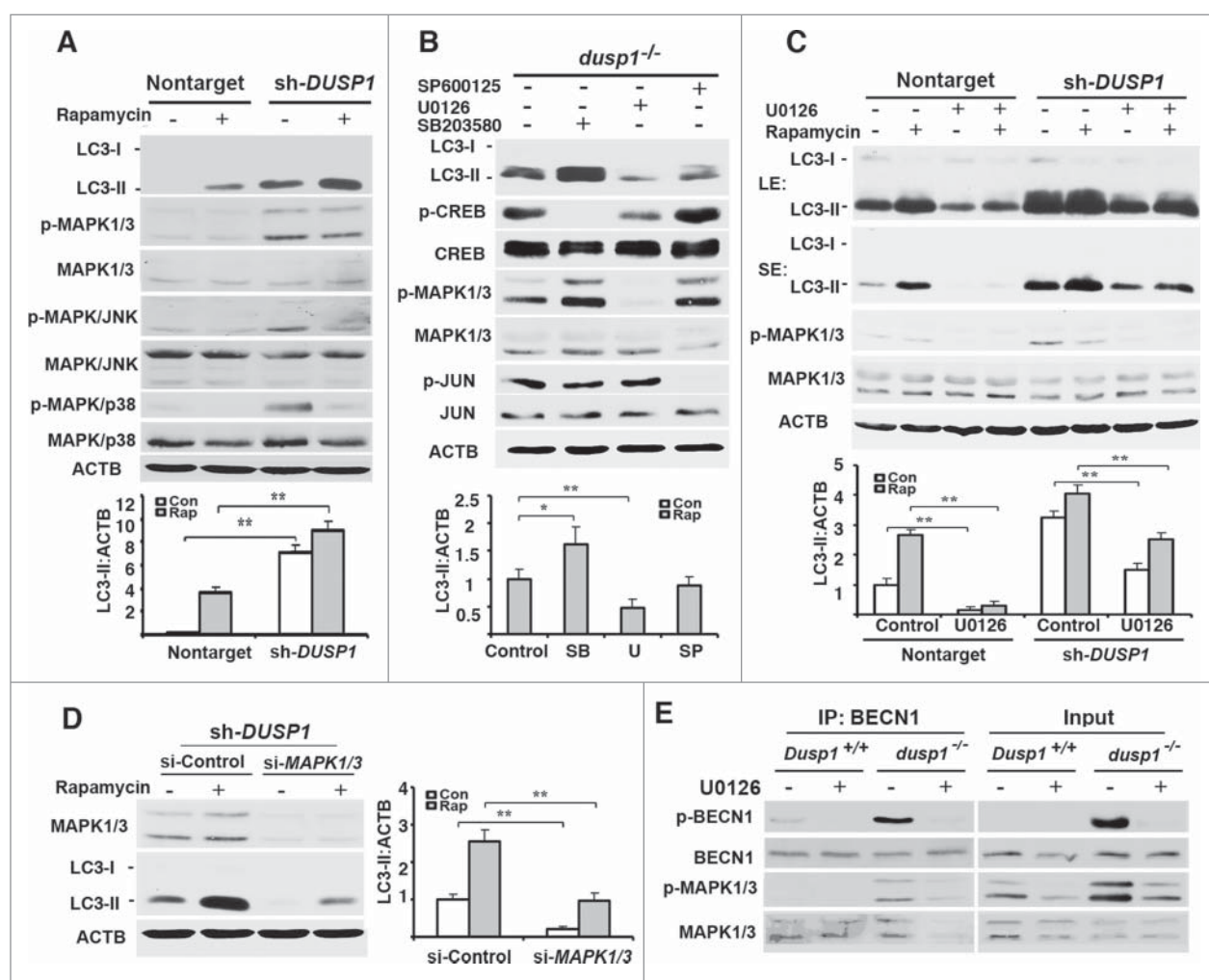


Figure 4. Effects of DUSP1 on MAPK activities and role of MAPKs in autophagy. (A) Western blot analyses of LC3, MAPK/p38, p-MAPK/p38, MAPK/ERK, p-MAPK/ERK, MAPK/JNK, and p-MAPK/JNK in control nontarget shRNA (nontarget) and *DUSP1* shRNA (sh-*DUSP1*) CAOV3 cells (upper panel) and quantification of LC3 (lower panel). Cells were left untreated or treated with 5 μ M rapamycin for 20 h prior to being harvested. (B) Western blot analyses of LC3, CREB, p-CREB, MAPK/ERK, p-MAPK/ERK, JUN and p-JUN in *dusp1*^{-/-} MEFs treated with MAPK inhibitors (upper panel) and quantification of LC3 (lower panel). Cells were left untreated or treated with 10 μ M SP600125 (SP), 10 μ M U0126 (U) or 5 μ M SB203580 (SB) for 24 h prior to being harvested for western blot analyses. (C) Western blot analyses of LC3, MAPK/ERK, and p-MAPK/ERK in nontarget and sh-*DUSP1* CAOV3 cells treated with rapamycin (5 μ M, 20 h), in the presence or absence of 10 μ M U0126 (upper panel); LE, long exposure; SE, short exposure) and quantification of LC3 (lower panel). (D) Western blot analyses of MAPK/ERK and LC3 in sh-*DUSP1* CAOV3 cells transfected with control siRNA (si-Control) or *MAPK1*-*MAPK3* siRNA (si-*MAPK1/3*) (left panel) and quantification of LC3 (right panel). Cells were left untreated or treated with 5 μ M rapamycin for 20 h prior to being harvested. (E) *Dusp1*^{+/+} and *dusp1*^{-/-} MEFs were left untreated or treated with U0126 and then harvested for immunoprecipitation (IP) with antibody to BECN1. Immunoprecipitated proteins were analyzed by western blot with anti-BECN1, BECN1 phosphorylated at Ser15 (p-BECN1), phosphorylated MAPK/ERK and total MAPK/ERK. Whole cell lysates were used as input control. Data in (A-D) represent mean \pm SD of 3 independent experiments. *, $P < 0.01$ and **, $P < 0.005$, statistically significant.

rapamycin-induced LC3-II levels in both nontarget and *DUSP1* shRNA knockdown CAOV3 cells (Fig. 4C). Comparable results were obtained if we knocked down *MAPK/ERK* by siRNA (Fig. 4D). Specifically, knocking down *MAPK/ERK* expression reduced both basal and rapamycin-induced LC3-II levels. Importantly, the phosphorylation of BECN1 at Ser15, a post-translational modification critical to BECN1's role in initiating autophagy,⁴³ was significantly increased in *dusp1*^{-/-} MEFs, as compared to *Dusp1*^{+/+} MEFs (Fig. 4E). Moreover, *Dusp1* knockout enhanced the association of BECN1 and phosphorylated MAPK/ERK, and the inhibition of MAP2K activity by U0126 significantly decreased the association of p-BECN1 (Ser15) and phosphorylated active MAPK/ERK (Fig. 4E). Collectively, these data suggest that *MAPK/ERK* activity plays a positive role in autophagy and that *DUSP1* targets *MAPK/ERK* to inhibit *MAPK/ERK*-mediated autophagy.

Dusp1 knockout promotes autophagy through ULK-mediated formation/activation of an ATG14-BECN1-PIK3C3 complex

To understand the mechanism by which *Dusp1* knockout or knockdown promotes autophagy, we first examined if *MTOR* (mechanistic target of rapamycin [serine/threonine kinase]), a well-characterized suppressor of the initiation of autophagy,⁴⁴ is altered in *dusp1*^{-/-} MEFs. *RPS6KB/p70S6K* is a downstream substrate of *MTOR* kinase, and its phosphorylation at Thr389 by *MTOR* is commonly used as a surrogate index of *MTOR* activity. As shown in Figure 5A, phospho-RPS6KB (at Thr389) was detected in both *Dusp1*^{+/+} and *dusp1*^{-/-} cells, and phosphorylation at Thr389 was inhibited by treatment with rapamycin, an inhibitor of *MTOR* activity. We detected in *dusp1*^{-/-} cells, but not *Dusp1*^{+/+} cells, increased phosphorylation of *ULK1* at Ser555 (Fig. 5B), which is a pro-autophagic activating

post-translational modification.⁴⁵ Levels of phosphorylated (p)-*BECN1* (at Ser15), a site phosphorylated by *ULK1*,⁴³ were also increased in *dusp1*^{-/-} cells (Fig. 5B). Knockdown of *Mapk1-Mapk3* by their siRNAs in *dusp1*^{-/-} MEFs significantly decreased basal and rapamycin-induced p-*ULK1* (Ser555) and p-*BECN1* (Ser15) levels (Fig. 5C). These data suggest that the activation of *BECN1* by phosphorylation at Ser15 in part depends on *MAPK/ERK* activity.

Increased levels of p-*ULK1* (Ser555), and p-*BECN1* (Ser15) in *dusp1*^{-/-} cells are conducive to the formation and activation of *PIK3C3* complexes needed for initiation of autophagosome formation.^{43,45,46} Coprecipitation analyses indicated that antibodies to *PIK3C3* pulled down increased amounts of *ATG14* and p-*BECN1* (Ser15) in *dusp1*^{-/-} cells, relative to *Dusp1*^{+/+} cells (Fig. 6A). These increases were observed under basal conditions, as well as after rapamycin treatment. Furthermore, activated *MAPK1/ERK2* and *MAPK3/ERK1* coprecipitated with the *PIK3C3*-*BECN1*-*ATG14* complexes (Fig. 6A). Importantly, knockdown of *Mapk1-Mapk3* in *dusp1*^{-/-} MEFs decreased *PIK3C3*-associated p-*BECN1* (S15) and *ATG14* complexes (Fig. 6B). In addition, we found that U0126 inhibits *Dusp1* knockout-induced LC3 punctate staining (Fig. 6C), and that overexpression of a constitutively active *Map2k1* itself, an upstream activator of *MAPK/ERK*, is sufficient to increase the accumulation of LC3 punctate structures (Fig. 6D). Thus, these data strongly suggest that *MAPK/ERK* promotes autophagy by affecting the formation of *PIK3C3*-*BECN1*-*ATG14* complexes.

Cisplatin-resistant ovarian cancer cells upregulate DUSP1 expression and are resistant to rapamycin

DUSP1 is often upregulated in cancer cells as they acquire resistance to chemotherapeutics such as cisplatin.^{32,47} We established a cisplatin-resistant CAOV3 cell line (i.e., CAOV3-

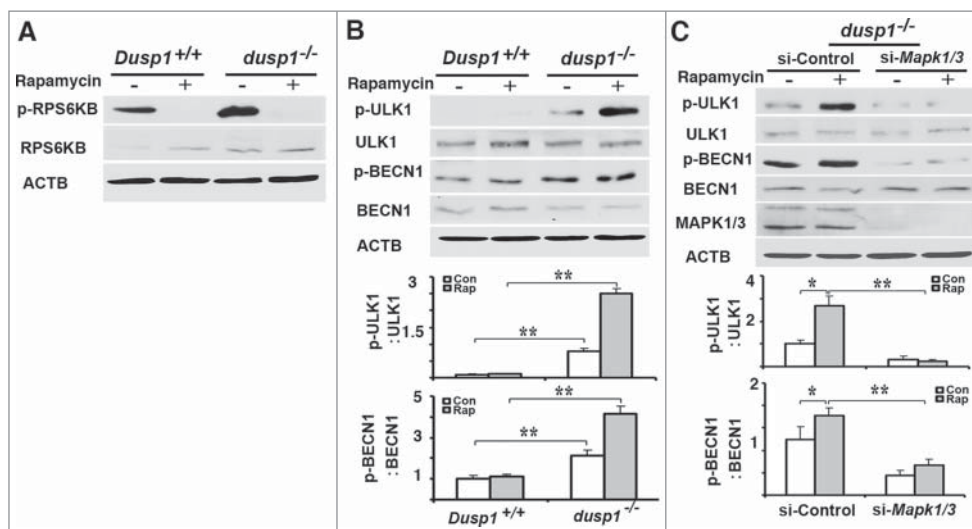


Figure 5. Effects of *DUSP1* on *RPS6KB*, *ULK1*, and *BECN1* phosphorylation. (A) Western blot analyses of the levels of total and phosphorylated *RPS6KB* (at Thr389) in *Dusp1*^{+/+} and *dusp1*^{-/-} MEFs. Cells were left untreated or treated with 5 μ M rapamycin for 20 h prior to being harvested. (B) Western blot analyses of the levels of p-*ULK1* (at Ser555), *ULK1*, p-*BECN1* (at Ser15) and *BECN1* (upper panel), and quantification of p-*ULK1* (Ser555) (middle panel) and p-*BECN1* (Ser15) (lower panel). *Dusp1*^{+/+} and *dusp1*^{-/-} MEFs were left untreated or treated with 5 μ M rapamycin for 20 h prior to being harvested. (C) Western blot analyses of the levels of p-*ULK1*, *ULK1*, p-*BECN1*, *BECN1* and *MAPK1*-*MAPK3* in *dusp1*^{-/-} MEFs (upper panel), and quantification of p-*ULK1* (middle panel) and p-*BECN1* (lower panel). Cells transfected with control siRNA (si-Control) or siRNA against *Mapk1/3* (si-*Mapk1/3*) were left untreated or treated with 5 μ M rapamycin for 20 h prior to being harvested. Data represent mean \pm SD of 3 independent experiments. *, $P < 0.01$ and **, $P < 0.005$, statistically significant.

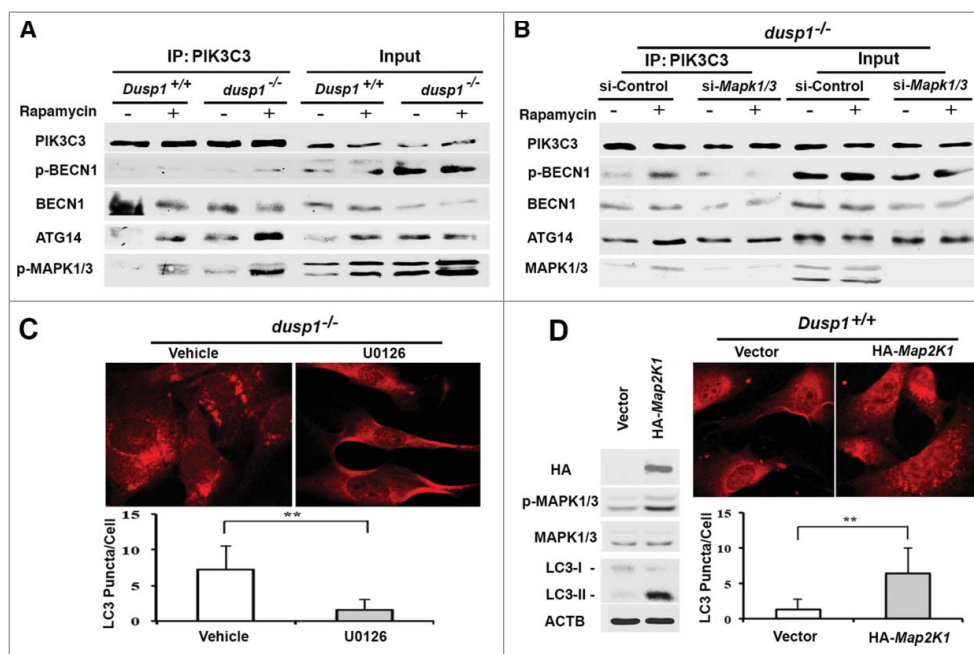


Figure 6. Effects of DUSP1 and MAPK/ERK on the association of PIK3C3, BECN1, ATG14, and p-MAPK/ERK. (A) *Dusp1*^{+/+} and *dusp1*^{-/-} MEFs were left untreated or treated with 5 μ M rapamycin for 20 h. Cell lysates were prepared, subjected to immunoprecipitation with antibody to PIK3C3, and then followed by western blot analyses using antibodies against BECN1, p-BECN1 (Ser15), ATG14 and p-MAPK1/ERK2-MAPK3/ERK1. Total cell lysates were used to assess input. (B) *Dusp1*^{-/-} MEFs were transfected with control siRNA (si-Control) or siRNA against Mapk1-Mapk3 (si-*Mapk1/3*), and treatments as well as IP-western blot were performed as in (A). (C) *Dusp1*^{-/-} MEFs were treated with 10 μ M U0126 for 24 h prior to being processed for immunofluorescent detection of LC3. Red fluorescent puncta denote autophagic vesicle structures (upper panel) and were quantified (lower panel). (D) *Dusp1*^{+/+} MEFs transfected with pMCL-*HA-Map2k1-R4F* or control vector for 24 h were used for western blot analyses of HA, p-MAPK/ERK, MAPK/ERK, LC3 and ACTB (left panel) and immunofluorescent detection of LC3 (upper right panel). The lower right panel depicts quantification of red fluorescent puncta. The data in (C and D) represent means \pm SD of analyses of minimally 20 cells. **, $P < 0.005$, statistically significant.

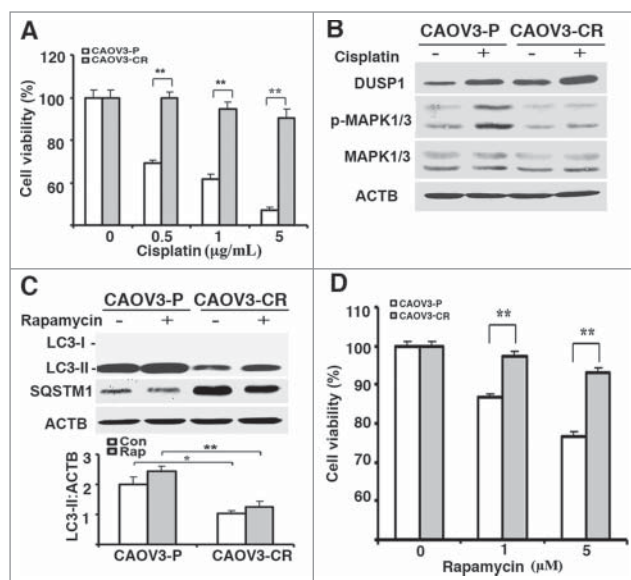


Figure 7. Cisplatin-resistant cells express high levels of DUSP1, low levels of activated MAPK/ERK and LC3-II, and decreased sensitivity to rapamycin. (A) CAOV3-P and CAOV3-CR cells were treated with different amounts of cisplatin for 48 h prior to being analyzed by MTT assays. (B) Western blot analyses of DUSP1 and MAPK/ERK in CAOV3-P and CAOV3-CR cells. Cells were left untreated or treated with 10 μ M cisplatin for 20 h before being harvested. (C) Cisplatin-resistant cells have a reduced capacity for autophagy. CAOV3-P and CAOV3-CR cells were left untreated or treated with 5 μ M rapamycin for 20 h prior to being harvested for western blot analyses of LC3 and SQSTM1 (upper panel) and quantification of LC3 (lower panel). (D) Cisplatin-resistant cells are less sensitive to rapamycin. CAOV3-P and CAOV3-CR cells were treated with the indicated doses of rapamycin for 48 h prior to MTT assays. Data represent mean \pm SD of 3 independent experiments. *, $P < 0.01$ and **, $P < 0.005$, statistically significant.

CR) by selection with increasing cisplatin doses over a 6-month period (Fig. 7A). Compared to parental CAOV3-P cells, CAOV3-CR cells expressed higher levels of both basal and cisplatin-induced DUSP1, and lower levels of cisplatin-induced phosphorylated MAPK/ERK (Fig. 7B). Importantly, CAOV3-CR cells expressed lower basal and rapamycin-induced accumulations of LC3-II and higher SQSTM1 levels than CAOV3-P cells (Fig. 7C). These data are consistent with the results obtained from TOV112D cells (Fig. 1C,F) in which overexpression of *DUSP1* suppressed both basal and inducible autophagy. In addition, we asked if the antiproliferative activities of rapamycin are dependent on the induction of autophagy. Figure 7D shows that CAOV3-P cells were more sensitive than CAOV3-CR cells to rapamycin, as scored in an MTT assay (Fig. 7D), as well as in a cell counting assay (data not shown).

To further define the role of DUSP1 in modulating the sensitivity of CAOV3 cells to rapamycin we transfected CAOV3-CR and CAOV3-P cells with nontarget or *DUSP1* siRNAs. Figure 8A shows that knockdown of *DUSP1* in CAOV3-CR cells facilitated MAPK/ERK activation and greatly enhanced rapamycin-mediated accumulation of LC3-II. A similar result was obtained with MEFs transfected with *Dusp1* siRNA (Fig. 8B). MTT assays indicated the *DUSP1* knockdown enhanced the effects of rapamycin in CAOV3-P cells, and sensitized previously resistant CAOV3-CR cells to rapamycin (Fig. 8C).

Discussion

Previous studies have implicated MAPK/ERK, MAPK/JNK and MAPK/p38 as being involved in, or a modifier of

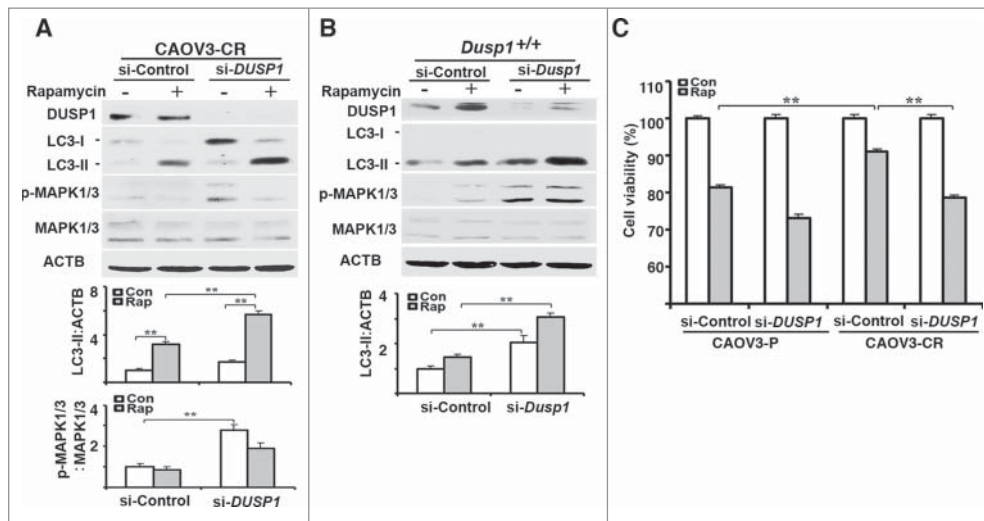


Figure 8. DUSP1-mediated suppression of autophagy is associated with cisplatin resistance in human ovarian cancer cells. (A) Effect of *DUSP1* knockdown on LC3 level in cisplatin-resistant ovarian cancer cells. CAOV3-CR cells were transfected with control nontarget siRNA (si-Control) or siRNA against *DUSP1* (si-DUSP1). Three days later the cells were either left alone or treated with 5 μ M rapamycin for 20 h prior to being harvested for western blot analyses of DUSP1, MAPK/ERK, and LC3 (upper panel), quantifications of LC3 (middle panel) and p-MAPK/ERK (lower panel). (B) Effect of *DUSP1* knockdown on LC3 level in MEFs. *Dusp1*^{+/+} MEFs were transfected with siRNA against *Dusp1* (si-Dusp1) or control nontarget siRNA (si-Control) and treated with rapamycin as in (A). DUSP1, MAPK/ERK, and LC3 were determined by western blot analysis (upper panel) and LC3-II was quantified (lower panel). (C) Effect of DUSP1 on rapamycin sensitivity. CAOV3-P and CAOV3-CR cells were transfected with *DUSP1* siRNA or control nontarget siRNA as in (A), and then left alone or treated with 5 μ M rapamycin for 48 h prior to harvesting for MTT assays. Data represent mean \pm SD of 3 independent experiments. **, $P < 0.005$, statistically significant.

autophagy.¹⁷⁻¹⁹ However, it was not known if their endogenous negative regulator, DUSP1, also plays a role in autophagy. In this study, we used multiple parameters to monitor autophagy and showed in 3 different cell model systems that knockdown or knockout of *DUSP1* increased constitutive/basal and rapamycin-inducible autophagy; whereas overexpression of *DUSP1* had opposite effects. Our data strongly suggest that DUSP1 negatively regulates autophagy.

Because knockdown or knockout of *DUSP1* enhanced both inducible and constitutive autophagy, and MAPKs are the only known substrates for DUSP1,^{35,42} these findings suggest that DUSP1 must act on MAPKs to inhibit autophagy. The role of individual MAPKs in autophagy is variable, and possibly cell-context dependent. Knockdown and inhibitor studies suggest that MAPK/ERK is necessary for the induction of autophagy in some cell models,^{19,48} but that elevated, persistent activity can suppress autophagosome maturation.⁴⁹ MAPK/JNK appears to be a positive modulator of autophagy via its ability to phosphorylate BCL2 and BCL2L1/BCL-XL, thus disrupting BCL2-BECN1 binding and facilitating BECN1 interaction with the PIK3C3 complex, which is required for initiation of phagophore formation.^{50,51} As for MAPK/p38, reports have appeared indicating that it is both an activator^{17,18,52} and inhibitor^{53,54} of autophagy. In this study, we showed that *DUSP1* knockdown increased the level of phosphorylated/activated MAPK/ERKs, MAPK/JNKs and MAPK/p38. Of the 3 MAPKs, only inhibition of MAPK/ERK by the MAP2K inhibitor U0126 strongly suppressed autophagy in *DUSP1* knockdown cells, a result that was confirmed by knockdown with siRNAs against *MAPK1/ERK2-MAPK3/ERK1*. In addition, we found that rapamycin-induced autophagy was abolished by U0126 or *MAPK/ERK* knockdown by siRNAs. Thus, we conclude that the enhancement of both basal and inducible autophagy by downregulating *DUSP1* reflects, at least in part, a MAPK/ERK-dependent process.

The increased basal and rapamycin-induced autophagic activity in *dusp1*^{-/-} cells, relative to *Dusp1*^{+/+} cells, correlated with increased content of the PIK3C3-BECN1-ATG14 complex. This complex is responsible for the initiation of phagophore formation. Furthermore, the BECN1 associated with the complex was phosphorylated at a site that enhances PIK3C3 kinase activity. Hence, the elevated autophagic activity observed in *dusp1*^{-/-} cells reflects, at least in part, a greater capacity for initiating phagophore formation. Interestingly, coprecipitation studies indicated that phosphorylated/active MAPK/ERKs were a component of the PIK3C3-BECN1-ATG14 complex. We currently do not know the role MAPK/ERKs play in this complex, which is under investigation.

ULK1 activity plays a critical role in the generation/activation of the PIK3C3 complex needed to initiate phagophore formation. The activity of ULK1 is negatively regulated by MTOR, and inhibition of MTOR activates ULK, leading to autophagy induction.⁴³ In the current study, *dusp1*^{-/-} cells exhibited elevated levels of phosphorylated ULK1 (at Ser555) and BECN1 (at Ser15). In essence, ULK1 phosphorylates BECN1 at Ser15 and promotes PIK3C3-BECN1-ATG14 complex formation and activation in *dusp1*^{-/-} cells. Given that enhanced autophagy occurred in *dusp1*^{-/-} cells, which could be suppressed by pharmacological inhibition or knockdown of MAPK/ERKs, it seems that ULK1 activation in *dusp1*^{-/-} cells is related to elevated MAPK/ERK activity.

An interesting outcome of the MAPK inhibitor studies was that treatment with the MAPK/p38 inhibitor SB203580 markedly enhanced the basal accumulation of LC3-II in *DUSP1*-deficient cells. This result is consistent with the effects of the MAPK/p38 inhibitor SB202190 in colon cancer cells,^{54,55} and suggests that MAPK/p38-mediated signaling may suppress basal autophagy. Since both MAPK/ERK and MAPK/p38 activities are increased in *DUSP1*-deficient CAOV3 cells (Fig. 4A), the observed increase in basal autophagy most likely represents

an aggregate of the 2 activities in which MAPK/ERK signaling predominates. Notably, the situation is less complicated in the case of rapamycin-induced autophagy in *DUSP1*-deficient cells since active MAPK/p38 levels were reduced in rapamycin-treated cells.

MTOR is both an inhibitor of autophagy and an activator of processes necessary for protein synthesis and cell division. As such, inhibitors of MTOR such as rapamycin are used as inducers of autophagy or as cancer therapeutics. Indeed, rapamycin and its analogs have been used as a single modality, and in combinational protocols, in the treatment of many forms of cancer, including ovarian cancer.^{56,57} In our studies rapamycin suppressed the proliferation of ovarian CAOV3 cells in a concentration-dependent fashion. Knockdown of *DUSP1* induced autophagy and markedly enhanced the efficacy of rapamycin's cytostatic effects. Thus, rapamycin-mediated induction of autophagy appears to contribute to the therapeutic properties of rapamycin in CAOV3 cells. We do not know the mechanism by which autophagy contributes to rapamycin's effects on cell viability. However, several studies have implicated autophagy as having a role in mediating the antiproliferative properties of some therapeutics.^{5,40}

Previous studies showed that *DUSP1* can be induced by cisplatin and that its induction contributes to cisplatin resistance.^{33,37,38} Consistent with these findings, we observed that basal levels of *DUSP1* were higher and MAPK/ERK activities were lower in cisplatin-resistant CAOV3-CR cells compared to the parental cells from which they were derived. Furthermore, basal and rapamycin-induced autophagy were markedly reduced in CAOV3-CR cells, as indicated by reduced LC3-II and elevated SQSTM1 levels. Because knockdown of *DUSP1* in CAOV3-CR cells increased basal and rapamycin-induced LC3-II levels, it appears that *DUSP1* plays a negative role in regulating autophagy in ovarian cancer cells that have developed acquired cisplatin resistance. Then, the question becomes what advantage does reducing autophagy provide CAOV3-CR cells. We speculate that the reduced capacity for autophagy in the CAOV3-CR cell line may be a secondary consequence (albeit a negative one) of the prosurvival mechanisms that were preferentially selected during continual exposure to cisplatin. For example, cisplatin causes the activation of MAPK/ERK, MAPK/JNK and MAPK/p38 in OV433 and 2008 ovarian cancer cells.^{40,58} Apoptosis occurring in 2008 ovarian cancer cells following cisplatin treatment can be suppressed by cotreatment with MAPK/JNK and MAPK/p38 inhibitors.⁵⁸ Interestingly, the anti-apoptotic activities of BCL2 are reduced/eliminated by its phosphorylation at Ser87 and Thr56 by MAPK/p38,⁵⁹ and at Ser70 by MAPK/JNK.⁶⁰ Given that *DUSP1* dephosphorylates and inactivates MAPK/ERK, MAPK/JNK and MAPK/p38, its overexpression would help preserve the anti-apoptotic activities of BCL2, but inadvertently suppress autophagy in CAOV3-CR cells due to an inhibition of MAPK/ERK activity.

We have also shown that knockdown of *DUSP1* markedly enhanced the sensitivity of CAOV3-CR cells to the antigrowth activities of rapamycin. The antigrowth properties of rapamycin can be attributable to not only its effects on protein translation, but also its ability to activate MAP3K5/ASK1- MAPK/JNK-mediated apoptosis in cells with mutant TP53/p53.⁶¹ The parental line from which CAOV3-CR cells were derived has a mutated TP53 that results in chain termination at codon 136.⁶²

Presumably, knockdown of *DUSP1* in the CAOV3-CR cell line would facilitate activation of the MAP3K5 pathway. Irrespective of the basis for why *DUSP1* knockdown sensitized CAOV3-CR cells to cisplatin, our finding is significant since ovarian tumors commonly develop resistance to cisplatin, and rapamycin analogs are increasingly being used as anticancer agents for ovarian cancer.^{56,57} Suppression of *DUSP1* activity or expression may be a means to potentiate the therapeutic activity of rapamycin analogs in cancer clinical trials.

In summary, this study makes the following novel observations: 1) *DUSP1* negatively regulates autophagy mediated by MAPK/ERKs; 2) the antigrowth activity of rapamycin on ovarian cancer cells is autophagy dependent; and 3) autophagy is suppressed by *DUSP1* in ovarian cancer cells that have developed acquired cisplatin resistance. Recognition that *DUSP1* inhibits autophagy is fundamental to our understanding of the mechanisms involved in the regulation of autophagy.

Materials and methods

Reagents

Cisplatin (P4394), bafilomycin A₁ (B1793) and anti-ACTB antibody (AC-74) were purchased from Sigma. Rapamycin (13346) was purchased from Cayman. Rabbit polyclonal *DUSP1* antibody (SC-370) was purchased from Santa Cruz Biotechnology. Rabbit antibodies against SQSTM1 (5114), LC3 (2775), ATG5 (2630), and total and phosphorylated MAPK/ERK (9102 and 9104), MAPK/p38 (9212 and 9211), MAPK/JNK (9252 and 9251), CREB (9197 and 9198), JUN (9165 and 9164), RPS6KB (9202 and 9205), ULK1 (8054), p-ULK1 at Ser555 (5869), BECN1 (3738), p-BECN1 at Ser15 (13825), and PIK3C3/VPS34 (4263) were purchased from Cell Signaling Technology. Antibody against ATG14 (PD016) was purchased from MBL. Mouse antibody against SQSTM1 (ab56416) was purchased from Abcam. E64d (324890) was purchased from EMD Millipore. The constitutively active mutant *Map2k1* plasmid (pMCL-HA-*Map2k1*-R4F) was kindly provided by Dr. Raymond Mattingly (Wayne State University), as described previously.⁶³

Cell lines, culture conditions and treatment

The human ovarian cancer cell lines TOV112D and CAOV3 were described previously.⁶⁴ Cell lines were maintained in MCDB105/M199 (Sigma, M2154 and M6395) or DMEM (Gibco, 12800-017), supplemented with 10% fetal bovine serum (Sigma, F2442) and antibiotics at 37°C in a humidified atmosphere consisting of 5% CO₂ and 95% air. *Dusp1* knockout MEFs (*dusp1*^{-/-} MEFs) and their matched wild-type MEFs (*Dusp1*^{+/+} MEFs) were described previously.³⁷

Construction of *DUSP1*-expressing vectors and generation of *DUSP1*-overexpression and *DUSP1*-knockdown cell lines

A full-length *DUSP1* cDNA was amplified from pIRES2-EGFP as described⁶⁵ using a GC-rich PCR system (Roche Applied Science, 12140306001) and the following primers: 5'-GGAATTCATGGTCATGGAAGTGGGC-3' and 5'-CGGGATCCTCA

GCAGCTGGGAGAGG-3'. The PCR conditions were as follows: 95°C for 3 min; 10 cycles at 95°C for 30 sec, 62°C for 30 sec, and 72°C for 135 sec, and then 25 cycles at 95°C for 30 sec, 62°C for 30 sec, and 72°C for 215 sec. The amplified fragment was isolated from a 1% agarose gel, digested with BamHI and EcoRI and subcloned into pNTAP (Stratagene, 240101) to generate pNTAP-*DUSP1*. To generate *DUSP1* stable expression cells, TOV112D cells were transfected with either pNTAP or pNTAP-*DUSP1* using Lipofectamine 2000 reagent (Invitrogen, 11668027). Transfected cells were selected with 800 $\mu\text{g}/\text{mL}$ G418 (Life Technologies, 10131027) for 4 wk, and individual clones were isolated as described elsewhere.³⁰ To generate cell lines whose *DUSP1* was stably knocked down, CAOV3 cells were transfected with *DUSP1* shRNA (SHGLY) or nontarget shRNA control vector (SHC002) from Sigma and selected by growth in medium containing 0.15 $\mu\text{g}/\text{mL}$ puromycin. Western blot analyses were used to identify clones that either had markedly elevated or reduced levels of *DUSP1*.

Generation of cisplatin-resistant CAOV3 cells

Parental CAOV3 cells (CAOV3-P) were gradually exposed to increased concentrations of cisplatin starting from 0.1 to 0.8 $\mu\text{g}/\text{mL}$ for over 6 mo to select cisplatin-resistant cells (CAOV3-CR), as described previously.⁴⁷

Electron microscopy

Cells were fixed with 0.1 M phosphate buffer (pH 7.2) containing 2.5% glutaraldehyde at room temperature for 2 h and then post-fixed with 1% osmium tetroxide for 90 min. The fixed cell pellets were dehydrated in graded ethanol and then embedded in 100% eponate resin (TED PELLA, INC, 18010). Tissue blocks were sectioned to a thickness of 80 nm and placed on 200 mesh rhodium/copper grids (Ernest F Fullam, Inc., 62130). The grids were counterstained with saturated uranyl acetate and lead citrate. The sections were then examined under a Zeiss EM 900 electron microscope (Carl Zeiss AG). Cells with double-membrane vacuoles and an intact nucleus were recorded as autophagic cells.

Knockdown of *DUSP1*, *MAPK1/ERK2-MAPK3/ERK1* and *Mapk1-Mapk3* expression by short interfering RNA (siRNA)

On-TARGETplus SMARTpool siRNAs for *DUSP1* (L-003484-02), *Dusp1* (M-040753-01), *MAPK1/ERK2-MAPK3/ERK1* (L-003555-00/L-003592-00), *Mapk1/Erk2-Mapk3/Erk1* (M-040126-01/M-040613-01) and corresponding control nontarget siRNAs (D-001810-10) were purchased from Dharmacon Research. The transfection was performed as suggested by the manufacturer's instructions with slight modifications, as described previously.⁴⁰ Briefly, cells were plated at 6×10^5 cells per well in 6-well plates. The next day, cells were transfected with *DUSP1* siRNA, *MAPK1-MAPK3* siRNA, *Mapk1-Mapk3* siRNA, or nontarget control siRNA using Lipofectamine 2000. After 3 d, transfected cells were left untreated or treated with 5 μM rapamycin for 20 h, and then harvested for subsequent western blot analysis.

MTT assays

The MTT assay was performed in 96-well plates as previously described.⁴⁰ Typically, there were 4 wells per treatment group.

Detection of exogenous GFP-LC3 by direct fluorescence and endogenous LC3 by indirect immunofluorescence

Cells were transfected with a GFP-LC3 expression vector for 24 h and then selected with G418 for 3 wk. Cells stably expressing GFP-LC3 were obtained and live cell fluorescence was recorded under an inverted fluorescence microscope (Olympus IX70). To detect endogenous LC3 by indirect immunofluorescence, cells grown on chamber slides were fixed with 3.5% formaldehyde, followed by treatment with 0.2% Triton X-100 (Sigma, T8787) in phosphate-buffered saline (Life Technologies, 70-013-032) for 10 min. After incubation with 1% BSA (Sigma, A2153) for 30 min, cells were incubated with a primary rabbit antibody against LC3 at 4°C overnight. The slides were then incubated with Texas red-conjugated anti-rabbit secondary antibodies (ThermoFisher, T-2767) for 30 min. The resulting cells were then incubated with DAPI. The slides were mounted with a coverslip and sealed with nail polish. Fluorescence was observed under a Zeiss LSM780 confocal microscope. We scored 20 or more cells per experiment, in each of 3 independent experiments, for the quantification of fluorescent LC3 puncta.

Western blot analysis

Whole cell lysates were prepared as described previously⁶⁵ and protein concentration was determined using the Protein Assay Kit (Bio-Rad, 500-0006). Cell lysates (50 μg) were electrophoresed through 12% or 15% denaturing polyacrylamide gels and transferred to a PVDF membrane (Millipore, IPVH00010). The blots were probed or reprobed with primary antibodies, and bound antibody was detected using anti-rabbit or mouse HRP- or fluorescence-linked secondary antibodies (ThermoFisher, 35568 and Cell Signaling, 7076), and Enhanced Chemiluminescence (ECL) ECLplus Reagent (Pierce, 80196) or the Odyssey infrared imaging system (LI-COR Biosciences) according to the manufacturer's protocol.

Statistical analysis

Statistical analyses were performed using Student *t* test. The data are presented as the mean \pm SD, and *p* value < 0.05 was considered significant.

Abbreviations

BafA ₁	bafilomycin A ₁
BECN1	Beclin 1, autophagy related
CREB	cAMP response element binding protein
DUSP1/MKP-1	dual-specificity protein phosphatase 1
MAPK	mitogen-activated protein kinase
MAP1LC3/LC3	microtubule-associated protein 1 light chain 3
MAP2K/MKK/MEK	mitogen-activated protein kinase kinase

MEFs	mouse embryonic fibroblasts
MTOR	mechanistic target of rapamycin (serine/threonine kinase)
MTT	3-(4,5-dimethylthiazol-2-yl)-2,5-diphenyltetrazolium bromide
PIK3C3	phosphoinositide-3-kinase, class 3
PtdIns3K	class III phosphatidylinositol 3-kinase
SQSTM1/p62	sequestosome 1
shRNA	short hairpin RNA
siRNA	small interfering RNA

Disclosure of potential conflicts of interest

No potential conflicts of interest were disclosed.

Acknowledgments

We thank Dr. James Hatfield for assistance with the electron microscopy and Dr. Yusen Liu for helpful discussion.

Funding

This work was supported, in part, by National Institutes of Health Grant 1R21CA178111 through the NCI.

References

- Klionsky DJ. Autophagy: from phenomenology to molecular understanding in less than a decade. *Nat Rev Mol Cell Biol* 2007; 8:931-7; PMID:17712358; <http://dx.doi.org/10.1038/nrm2245>
- Klionsky DJ, Abeliovich H, Agostinis P, Agrawal DK, Aliev G, Askew DS, Baba M, Baehrecke EH, Bahr BA, Ballabio A, et al. Guidelines for the use and interpretation of assays for monitoring autophagy in higher eukaryotes. *Autophagy* 2008; 4:151-75; PMID:18188003; <http://dx.doi.org/10.4161/auto.5338>
- Scarlatti F, Maffei R, Beau I, Codogno P, Ghidoni R. Role of non-canonical Beclin 1-independent autophagy in cell death induced by resveratrol in human breast cancer cells. *Cell Death Differ* 2008; 15:1318-29; PMID:18421301; <http://dx.doi.org/10.1038/cdd.2008.51>
- Denton D, Nicolson S, Kumar S. Cell death by autophagy: facts and apparent artefacts. *Cell Death Differ* 2012; 19:87-95; PMID:22052193; <http://dx.doi.org/10.1038/cdd.2011.146>
- Sui X, Chen R, Wang Z, Huang Z, Kong N, Zhang M, Han W, Lou F, Yang J, Shang Q, et al. Autophagy and chemotherapy resistance: a promising therapeutic target for cancer treatment. *Cell Death Dis* 2013; 4:e838; PMID:24113172; <http://dx.doi.org/10.1038/cddis.2013.350>
- Aredia F, Ortiz LMG, Giansanti V, Scovassi AI. Autophagy and cancer. *Cells* 2012; 1:520-34; PMID:24710488; <http://dx.doi.org/10.3390/cells1030520>
- Mathew R, Kongara S, Beaudoin B, Karp CM, Bray K, Degenhardt K, Chen G, Jin S, White E. Autophagy suppresses tumor progression by limiting chromosomal instability. *Genes Dev* 2007; 21:1367-81; PMID:17510285; <http://dx.doi.org/10.1101/gad.1545107>
- Mathew R, Karp CM, Beaudoin B, Vuong N, Chen G, Chen HY, Bray K, Reddy A, Bhanot G, Gelinas C, et al. Autophagy suppresses tumorigenesis through elimination of P62. *Cell* 2009; 137:1062-75; PMID:19524509; <http://dx.doi.org/10.1016/j.cell.2009.03.048>
- Yue Z, Jin S, Yang C, Levine AJ, Heintz N. Beclin 1, an autophagy gene essential for early embryonic development, is a haploinsufficient tumor suppressor. *Proc Natl Acad Sci U S A* 2003; 100:15077-82; PMID:14657337; <http://dx.doi.org/10.1073/pnas.2436255100>
- Martinez-Outschoorn UE, Trimmer C, Lin Z, Whitaker-Menezes D, Chiavarina B, Zhou J, Wang C, Pavlides S, Martinez-Cantarín MP, Capozza F, et al. Autophagy in cancer associated fibroblasts promotes tumor cell survival: Role of hypoxia, HIF1 induction and NFκpA activation in the tumor stromal microenvironment. *Cell Cycle* 2010; 9:3515-33; PMID:20855962; <http://dx.doi.org/10.4161/cc.9.17.12928>
- Chiavarina B, Whitaker-Menezes D, Migneco G, Martinez-Outschoorn UE, Pavlides S, Howell A, Tanowitz HB, Casimiro MC, Wang C, Pestell RG, et al. HIF1-α functions as a tumor promoter in cancer associated fibroblasts, and as a tumor suppressor in breast cancer cells: Autophagy drives compartment-specific oncogenesis. *Cell Cycle* 2010; 9:3534-51; PMID:20864819; <http://dx.doi.org/10.4161/cc.9.17.12908>
- Davis RJ. Signal transduction by the JNK group of MAP kinases. *Cell* 2000; 103:239-52; PMID:11057897; [http://dx.doi.org/10.1016/S0092-8674\(00\)00116-1](http://dx.doi.org/10.1016/S0092-8674(00)00116-1)
- Johnson GL, Lapadat R. Mitogen-activated protein kinase pathways mediated by ERK, JNK, and p38 protein kinases. *Science* 2002; 298:1911-2; PMID:12471242; <http://dx.doi.org/10.1126/science.1072682>
- Pearson G, Robinson F, Beers Gibson T, Xu BE, Karandikar M, Berman K, Cobb MH. Mitogen-activated protein (MAP) kinase pathways: regulation and physiological functions. *Endocr Rev* 2001; 22:153-83; PMID:11294822
- Chang L, Karin M. Mammalian MAP kinase signalling cascades. *Nature* 2001; 410:37-40; PMID:11242034; <http://dx.doi.org/10.1038/35065000>
- Kennedy NJ, Davis RJ. Role of JNK in tumor development. *Cell Cycle* 2003; 2:199-201; PMID:12734425
- Moruno-Manchon JF, Perez-Jimenez E, Knecht E. Glucose induces autophagy under starvation conditions by a p38 MAPK-dependent pathway. *Biochem J* 2013; 449:497-506; PMID:23116132; <http://dx.doi.org/10.1042/BJ20121122>
- Matsuzawa T, Kim BH, Shenoy AR, Kamitani S, Miyake M, Macmicking JD. IFN-γ elicits macrophage autophagy via the p38 MAPK signaling pathway. *J Immunol* 2012; 189:813-8; PMID:22675202; <http://dx.doi.org/10.4049/jimmunol.1102041>
- Pattingre S, Bauvy C, Codogno P. Amino acids interfere with the ERK1/2-dependent control of macroautophagy by controlling the activation of Raf-1 in human colon cancer HT-29 cells. *The J Biol Chem* 2003; 278:16667-74; PMID:12609989; <http://dx.doi.org/10.1074/jbc.M210998200>
- Dickinson RJ, Keyse SM. Diverse physiological functions for dual-specificity MAP kinase phosphatases. *J Cell Sci* 2006; 119:4607-15; PMID:17093265; <http://dx.doi.org/10.1242/jcs.03266>
- Lau LF, Nathans D. Identification of a set of genes expressed during the G0/G1 transition of cultured mouse cells. *EMBO J* 1985; 4:3145-51; PMID:3841511
- Charles CH, Ablner AS, Lau LF. cDNA sequence of a growth factor-inducible immediate early gene and characterization of its encoded protein. *Oncogene* 1992; 7:187-90; PMID:1741163
- Keyse SM, Emslie EA. Oxidative stress and heat shock induce a human gene encoding a protein-tyrosine phosphatase. *Nature* 1992; 359:644-7; PMID:1406996; <http://dx.doi.org/10.1038/359644a0>
- Liu Y, Gorospe M, Yang C, Holbrook NJ. Role of mitogen-activated protein kinase phosphatase during the cellular response to genotoxic stress. Inhibition of c-Jun N-terminal kinase activity and AP-1-dependent gene activation. *J Biol Chem* 1995; 270:8377-80; PMID:7721728; <http://dx.doi.org/10.1074/jbc.270.15.8377>
- Sun H, Charles CH, Lau LF, Tonks NK. MKP-1 (3CH134), an immediate early gene product, is a dual specificity phosphatase that dephosphorylates MAP kinase in vivo. *Cell* 1993; 75:487-93; PMID:8221888; [http://dx.doi.org/10.1016/0092-8674\(93\)90383-2](http://dx.doi.org/10.1016/0092-8674(93)90383-2)
- Noguchi T, Metz R, Chen L, Mattei MG, Carrasco D, Bravo R. Structure, mapping, and expression of erp, a growth factor-inducible gene encoding a nontransmembrane protein tyrosine phosphatase, and effect of ERP on cell growth. *Mol Cell Biol* 1993; 13:5195-205; PMID:8355678; <http://dx.doi.org/10.1128/MCB.13.9.5195>
- Franklin CC, Kraft AS. Conditional expression of the mitogen-activated protein kinase (MAPK) phosphatase MKP-1 preferentially inhibits p38 MAPK and stress-activated protein kinase in U937 cells. *J Biol Chem* 1997; 272:16917-23; PMID:9202001; <http://dx.doi.org/10.1074/jbc.272.27.16917>
- Brondello JM, McKenzie FR, Sun H, Tonks NK, Pouyssegur J. Constitutive MAP kinase phosphatase (MKP-1) expression blocks G1

- specific gene transcription and S-phase entry in fibroblasts. *Oncogene* 1995; 10:1895-904; PMID:7761091
- [29] Wu GS. The functional interactions between the p53 and MAPK signaling pathways. *Cancer Bio Ther* 2004; 3:156-61; PMID:14764989; <http://dx.doi.org/10.4161/cbt.3.2.614>
- [30] Li M, Zhou JY, Ge Y, Matherly LH, Wu GS. The phosphatase MKP1 is a transcriptional target of p53 involved in cell cycle regulation. *J Biol Chem* 2003; 278:41059-68; PMID:12890671; <http://dx.doi.org/10.1074/jbc.M307149200>
- [31] Franklin CC, Srikanth S, Kraft AS. Conditional expression of mitogen-activated protein kinase phosphatase-1, MKP-1, is cytoprotective against UV-induced apoptosis. *Proc Natl Acad Sci USA* 1998; 95:3014-9; PMID:9501207; <http://dx.doi.org/10.1073/pnas.95.6.3014>
- [32] Sanchez-Perez I, Martinez-Gomariz M, Williams D, Keyse SM, Perona R. CL100/MKP-1 JNK activation and apoptosis in response to cisplatin. *Oncogene* 2000; 19:5142-52; PMID:11064451; <http://dx.doi.org/10.1038/sj.onc.1203887>
- [33] Chattopadhyay S, Machado-Pinilla R, Manguan-Garcia C, Beldaniesta C, Moratilla C, Cejas P, Fresno-Vara JA, de Castro-Carpeno J, Casado E, Nistal M, et al. MKP1/CL100 controls tumor growth and sensitivity to cisplatin in non-small-cell lung cancer. *Oncogene* 2006; 25:3335-45; PMID:16462770; <http://dx.doi.org/10.1038/sj.onc.1209364>
- [34] Wang HY, Cheng Z, Malbon CC. Overexpression of mitogen-activated protein kinase phosphatases MKP1, MKP2 in human breast cancer. *Cancer Lett* 2003; 191:229-37; PMID:12618338; [http://dx.doi.org/10.1016/S0304-3835\(02\)00612-2](http://dx.doi.org/10.1016/S0304-3835(02)00612-2)
- [35] Wu GS. Role of mitogen-activated protein kinase phosphatases (MKPs) in cancer. *Cancer Metastasis Rev* 2007; 26:579-85; PMID:17717636; <http://dx.doi.org/10.1007/s10555-007-9079-6>
- [36] Rojo F, Gonzalez-Navarrete I, Bragado R, Dalmasas A, Menendez S, Cortes-Sempere M, Suarez C, Oliva C, Servitja S, Rodriguez-Fanjul V, et al. Mitogen-activated protein kinase phosphatase-1 in human breast cancer independently predicts prognosis and is repressed by doxorubicin. *Clin Cancer Res* 2009; 15:3530-9; PMID:19417026; <http://dx.doi.org/10.1158/1078-0432.CCR-08-2070>
- [37] Wang Z, Xu J, Zhou JY, Liu Y, Wu GS. Mitogen-activated protein kinase phosphatase-1 is required for cisplatin resistance. *Cancer Res* 2006; 66:8870-7; PMID:16951204; <http://dx.doi.org/10.1158/0008-5472.CAN-06-1280>
- [38] Wang J, Zhou JY, Wu GS. ERK-dependent MKP-1-mediated cisplatin resistance in human ovarian cancer cells. *Cancer Res* 2007; 67:11933-41; PMID:18089824; <http://dx.doi.org/10.1158/0008-5472.CAN-07-5185>
- [39] Raught B, Gingras AC, Sonenberg N. The target of rapamycin (TOR) proteins. *Proc Natl Acad Sci U S A* 2001; 98:7037-44; PMID:11416184; <http://dx.doi.org/10.1073/pnas.121145898>
- [40] Wang J, Wu GS. Role of autophagy in cisplatin resistance in ovarian cancer cells. *J Biol Chem* 2014; 289:17163-73; PMID:24794870; <http://dx.doi.org/10.1074/jbc.M114.558288>
- [41] Yamamoto A, Tagawa Y, Yoshimori T, Moriyama Y, Masaki R, Tashiro Y. Bafilomycin A1 prevents maturation of autophagic vacuoles by inhibiting fusion between autophagosomes and lysosomes in rat hepatoma cell line, H-4-II-E cells. *Cell Struct Funct* 1998; 23:33-42; PMID:9639028; <http://dx.doi.org/10.1247/csf.23.33>
- [42] Keyse SM. Dual-specificity MAP kinase phosphatases (MKPs) and cancer. *Cancer Metastasis Rev* 2008; 27:253-61; PMID:18330678; <http://dx.doi.org/10.1007/s10555-008-9123-1>
- [43] Russell RC, Tian Y, Yuan H, Park HW, Chang YY, Kim J, Kim H, Neufeld TP, Dillin A, Guan KL. ULK1 induces autophagy by phosphorylating Beclin-1 and activating VPS34 lipid kinase. *Nat Cell Biol* 2013; PMID:23685627
- [44] Alers S, Loffler AS, Wesselborg S, Stork B. Role of AMPK-mTOR-Ulk1/2 in the regulation of autophagy: cross talk, shortcuts, and feedbacks. *Mol Cell Biol* 2012; 32:2-11; PMID:22025673; <http://dx.doi.org/10.1128/MCB.06159-11>
- [45] Tian W, Li W, Chen Y, Yan Z, Huang X, Zhuang H, Zhong W, Chen Y, Wu W, Lin C, et al. Phosphorylation of ULK1 by AMPK regulates translocation of ULK1 to mitochondria and mitophagy. *FEBS Lett* 2015; 589:1847-54; PMID:25980607; <http://dx.doi.org/10.1016/j.febslet.2015.05.020>
- [46] Fogel AI, Dlouhy BJ, Wang C, Ryu SW, Neutzner A, Hasson SA, Sideris DP, Abeliovich H, Youle RJ. Role of membrane association and Atg14-dependent phosphorylation in beclin-1-mediated autophagy. *Mol Cell Biol* 2013; 33:3675-88; PMID:23878393; <http://dx.doi.org/10.1128/MCB.00079-13>
- [47] Wang J, Zhou JY, Zhang L, Wu GS. Involvement of MKP-1 and Bcl-2 in acquired cisplatin resistance in ovarian cancer cells. *Cell Cycle* 2009; 8:3191-8; PMID:19755862; <http://dx.doi.org/10.4161/cc.8.19.9751>
- [48] Wang J, Whiteman MW, Lian H, Wang G, Singh A, Huang D, Denmark T. A non-canonical MEK/ERK signaling pathway regulates autophagy via regulating Beclin 1. *J Biol Chem* 2009; 284:21412-24; PMID:19520853; <http://dx.doi.org/10.1074/jbc.M109.026013>
- [49] Corcelle E, Nebout M, Bekri S, Gauthier N, Hofman P, Poujeol P, Fenichel P, Mograbi B. Disruption of autophagy at the maturation step by the carcinogen lindane is associated with the sustained mitogen-activated protein kinase/extracellular signal-regulated kinase activity. *Cancer Res* 2006; 66:6861-70; PMID:16818664; <http://dx.doi.org/10.1158/0008-5472.CAN-05-3557>
- [50] Wei Y, Pattingre S, Sinha S, Bassik M, Levine B. JNK1-mediated phosphorylation of Bcl-2 regulates starvation-induced autophagy. *Mol Cell* 2008; 30:678-88; PMID:18570871; <http://dx.doi.org/10.1016/j.molcel.2008.06.001>
- [51] Kang R, Zeh HJ, Lotze MT, Tang D. The Beclin 1 network regulates autophagy and apoptosis. *Cell Death Differ* 2011; 18:571-80; PMID:21311563; <http://dx.doi.org/10.1038/cdd.2010.191>
- [52] Paillas S, Causse A, Marzi L, de Medina P, Poirot M, Denis V, Vezzio-Vie N, Espert L, Arzouk H, Coquelle A, et al. MAPK14/p38alpha confers irinotecan resistance to TP53-defective cells by inducing survival autophagy. *Autophagy* 2012; 8:1098-112; PMID:22647487; <http://dx.doi.org/10.4161/auto.20268>
- [53] Keil E, Hocker R, Schuster M, Essmann F, Ueffing N, Hoffman B, Liebermann DA, Pfeffer K, Schultze-Osthoff K, Schmitz I. Phosphorylation of Atg5 by the Gadd45beta-MEKK4-p38 pathway inhibits autophagy. *Cell Death Differ* 2013; 20:321-32; PMID:23059785; <http://dx.doi.org/10.1038/cdd.2012.129>
- [54] Comes F, Matrone A, Lastella P, Nico B, Susca FC, Bagnulo R, Ingravallo G, Modica S, Lo Sasso G, Moschetta A, et al. A novel cell type-specific role of p38alpha in the control of autophagy and cell death in colorectal cancer cells. *Cell Death Differ* 2007; 14:693-702; PMID:17159917; <http://dx.doi.org/10.1038/sj.cdd.4402076>
- [55] Corcelle E, Djerbi N, Mari M, Nebout M, Fiorini C, Fenichel P, Hofman P, Poujeol P, Mograbi B. Control of the autophagy maturation step by the MAPK ERK and p38: lessons from environmental carcinogens. *Autophagy* 2007; 3:57-9; PMID:17102581; <http://dx.doi.org/10.4161/auto.3424>
- [56] Schlosshauer PW, Li W, Lin KT, Chan JL, Wang LH. Rapamycin by itself and additively in combination with carboplatin inhibits the growth of ovarian cancer cells. *Gynecol Oncol* 2009; 114:516-22; PMID:19576622; <http://dx.doi.org/10.1016/j.ygyno.2009.06.002>
- [57] Mabuchi S, Hisamatsu T, Kimura T. Targeting mTOR signaling pathway in ovarian cancer. *Curr Med Chem* 2011; 18:2960-8; PMID:21651485; <http://dx.doi.org/10.2174/092986711796150450>
- [58] Mansouri A, Ridgway LD, Korapati AL, Zhang Q, Tian L, Wang Y, Siddik ZH, Mills GB, Claret FX. Sustained activation of JNK/p38 MAPK pathways in response to cisplatin leads to Fas ligand induction and cell death in ovarian carcinoma cells. *J Biol Chem* 2003; 278:19245-56; PMID:12637505; <http://dx.doi.org/10.1074/jbc.M208134200>
- [59] De Chiara G, Marcocci ME, Torcia M, Lucibello M, Rosini P, Bonini P, Higashimoto Y, Damonte G, Armirotti A, Amodei S, et al. Bcl-2 Phosphorylation by p38 MAPK: identification of target sites and biologic consequences. *J Biol Chem* 2006; 281:21353-61; PMID:16714293; <http://dx.doi.org/10.1074/jbc.M511052200>
- [60] Srivastava RK, Mi QS, Hardwick JM, Longo DL. Deletion of the loop region of Bcl-2 completely blocks paclitaxel-induced apoptosis. *Proc*

- Natl Acad Sci U S A 1999; 96:3775-80; PMID:10097113; <http://dx.doi.org/10.1073/pnas.96.7.3775>
- [61] Huang S, Shu L, Dilling MB, Easton J, Harwood FC, Ichijo H, Houghton PJ. Sustained activation of the JNK cascade and rapamycin-induced apoptosis are suppressed by p53/p21(Cip1). *Mol Cell* 2003; 11:1491-501; PMID:12820963; [http://dx.doi.org/10.1016/S1097-2765\(03\)00180-1](http://dx.doi.org/10.1016/S1097-2765(03)00180-1)
- [62] Yaginuma Y, Westphal H. Abnormal structure and expression of the p53 gene in human ovarian carcinoma cell lines. *Cancer Res* 1992; 52:4196-9; PMID:1638534
- [63] Mansour SJ, Matten WT, Hermann AS, Candia JM, Rong S, Fukasawa K, Wande Woude GF, Ahn NG. Transformation of mammalian cells by constitutively active MAP kinase kinase. *Science* 1994; 265:966-70; PMID:8052857; <http://dx.doi.org/10.1126/science.8052857>
- [64] Kwong J, Lee JY, Wong KK, Zhou X, Wong DT, Lo KW, Welch WR, Berkowitz RS, Mok SC. Candidate tumor-suppressor gene DLEC1 is frequently downregulated by promoter hypermethylation and histone hypoacetylation in human epithelial ovarian cancer. *Neoplasia* 2006; 8:268-78; PMID:16756719; <http://dx.doi.org/10.1593/neo.05502>
- [65] Zhou JY, Liu Y, Wu GS. The role of mitogen-activated protein kinase phosphatase-1 in oxidative damage-induced cell death. *Cancer Res* 2006; 66:4888-94; PMID:16651445; <http://dx.doi.org/10.1158/0008-5472.CAN-05-4229>